Plant Cell, Tissue and Organ Culture (PCTOC) (2026) 164:92
https://doi.org/10.1007/s11240-026-03346-w

ORIGINAL ARTICLE

Aluminum tolerance in *Pfaffia glomerata* is associated with antioxidant defense, osmolyte accumulation, and pathway-specific transcriptional regulation

Michelle Maylla V. Almeida[1,7] · Tatiane D. Silva[1,7] · Quezia P. Dutra[1] · Luiza Eduarda G. Monteiro[1] · Marcus Dhilermando H. Souza[1] · Elisandra S. Sousa[1] · Joseila Maldaner[2] · Sérgio Heitor S. Felipe[3] · Juliane M. Henschel[4] · Diego S. Batista[4,6] · Evandro A. Fortini[1,7] · Auxiliadora O. Martins[5] · Wagner L. Araújo[5] · Wagner C. Otoni[1]

Received: 30 October 2025 / Accepted: 6 January 2026 / Published online: 3 March 2026
© The Author(s) 2026

Abstract

Aluminum (Al) contamination in acidic soils severely limits plant growth and development. This study investigated the mechanisms and timing of Al toxicity in *Pfaffia glomerata*, a medicinal species of growing pharmacological interest. Based on the hypothesis that *P. glomerata* mitigates Al toxicity through tissue-specific adjustments in redox metabolism, accumulation of protective metabolites, and regulation of genes involved in cell wall structure and 20-hydroxyecdysone biosynthesis, plantlets were grown in vitro for 40 days under five Al concentrations (0, 200, 400, 600, and 800 µM). Concentrations above 600 µM significantly impaired plant growth. Aluminum accumulated in both roots and leaves, indicating active translocation throughout the plant. Plants exposed to 600 µM Al exhibited increased levels of glucose and fructose, and to a lesser extent, sucrose and starch. Additionally, starch, proline, malate, and fumarate levels rose in response to Al stress, suggesting metabolic adjustments for stress mitigation. Elevated antioxidant enzyme activity and malondialdehyde accumulation in the roots indicated oxidative stress. At the molecular level, the expression of genes related to 20-hydroxyecdysone biosynthesis (*PgSpook* and *PgPhantom*) was downregulated in the roots, while genes involved in cell wall biosynthesis (*PgCCR*, *PgCAD*, *PgC4H*) were upregulated in the leaves and downregulated in the roots. These findings show that P. glomerata tolerates moderate Al stress via a multifaceted response involving morphological adjustments, redox regulation, metabolite accumulation, and differential gene expression. This is the first evidence of Al-induced downregulation of 20-hydroxyecdysone biosynthesis in a medicinal species and identifies novel molecular targets for enhancing stress tolerance in non-model plants.

Key message

Pfaffia glomerata tolerates aluminum toxicity through tissue-specific metabolic and transcriptional reprogramming, revealing novel links between aluminum stress and the downregulation of 20-hydroxyecdysone biosynthesis in a medicinal plant.

Keywords 20-hydroxyecdysone · Brazilian-ginseng · medicinal plants · Morphoanatomy · Oxidative stress · Proline

Introduction

The increase in soil acidity caused by extreme natural events and anthropogenic activities presents a severe problem for plant growth and sustainable agriculture (Chauhan et al. 2021; Zhang et al. 2019; Farooq et al. 2022; Ur Rahman et al. 2024). One of the main sources of acidity in soils with pH < 5 is the release of trivalent aluminum (Al^{3+}) (Chamier et al. 2015). Excess Aluminum (Al) in the soil disrupts physiological and metabolic processes by inhibiting cell division and root elongation and decreasing root hair formation. These changes prevent plants from absorbing

Communicated by Ming-Tsair Chan

Extended author information available on the last page of the article

sufficient water and essential nutrients, ultimately leading to a reduction in overall biomass (Nunes-Nesi et al. 2007; Rahman and Upadhyaya 2021; Hossain et al. 2023). Excess Al also triggers the overproduction of reactive oxygen species (ROS), promoting oxidative stress and peroxidation of membrane lipids (Singh et al. 2017; Chauhan et al. 2021).

Aluminum triggers changes in photosynthetic activity by altering CO_2 assimilation, stomatal conductance, and leaf transpiration (Sade et al. 2016; Bojórquez-Quintal et al. 2017; Singh et al. 2017; Cárcamo et al. 2019; Kar et al. 2021; Phukunkamkaew et al. 2021). Furthermore, Al can bind to the phosphodiester backbone of DNA and damage both the composition and replication of genetic material (Gupta et al. 2013; Singh et al. 2017; Phukunkamkaew et al. 2021). Plants employ various strategies to cope with Al toxicity, including the sequestration of Al in vacuoles; exudation of organic acids, such as citrate, oxalate, and malate from root apex cells (forming Al-organic acid complexes); activation of antioxidant machinery; and overexpression of genes responsive to Al stress (Ur Rahman et al. 2024).

Excess Al alters plant secondary metabolism, particularly pathways associated with phytoecdysteroid biosynthesis and phenylpropanoid metabolism. Phytoecdysteroids are bioactive compounds synthesized by plants, mainly as a defense against phytophagous insects (Das et al. 2021), and 20-hydroxyecdysone (20-E) is the predominant phytoecdysteroid in *Pfaffia glomerata*, a commercially important ginseng species cultivated in Brazil (Nascimento et al. 2007; Ribeiro et al.; Cotrim-Ribeiro et al. 2024). Due to its medicinal properties, 20-E is extracted from *P. glomerata* roots for phytopharmaceutical applications (Silva et al. 2021). The biosynthesis of 20-E is regulated by cytochrome P450 enzymes, including *Phantom* (CYP306A1) and *Spook* (CYP307A1), which catalyze key oxidative steps and represent regulatory control points of the pathway (Batista et al. 2019). In addition, Al stress strongly affects cell wall structure, prompting us to analyze genes of the phenylpropanoid pathway, including *PgC4H*, *PgCCoAOMT*, *PgCCR*, and *PgCAD*, which govern lignin biosynthesis and cell wall remodeling (Louback et al. 2021). The selection of these enzymes enables assessment of how Al stress coordinately modulates phytoecdysteroid production and cell wall–related metabolic responses in *P. glomerata*.

P. glomerata is a perennial species that exhibits moderate tolerance to several heavy metals, including Cd, Pb, Zn, As, and Al (Gupta et al. 2011, Calgaroto et al. 2010; Gomes et al. 2012, 2013 Gupta et al. 2013; Maldaner et al. 2015). However, while metal tolerance may allow cultivation in marginal or contaminated environments, the potential accumulation of metals such as Al in medicinal tissues remains a critical consideration for product safety and industrial application. To date, information on Al accumulation in *P. glomerata* tissues destined for medicinal use is limited, and whether Al exposure results in elevated Al content in derived products remains unclear. This knowledge gap highlights the importance of understanding how Al stress affects both secondary metabolite biosynthesis and metal partitioning, with direct implications for the phytopharmaceutical industry and quality control of *P. glomerata*-based products. Kamada et al. (2009) reported high divergence between *P. glomerata* individuals from different populations with respect to the content of specific phytoecdysteroids across tissues. Secondary metabolism (specialized metabolsim) and phytoecdysteroid production can be modulated also by ultraviolet B radiation (Felipe et al. 2019), moderate salt stress (Felipe et al. 2019), long photoperiods (Fortini et al. 2023), spectral quality (red and blue LEDs) (Silva et al. 2020), and irradiance (Silva et al. 2020b). The observed plasticity in secondary metabolism of different *P. glomerata* accessions may contribute to their greater tolerance of extreme environmental conditions.

P. glomerata plants can be found in soils rich in Al such as the Cerrado Biome. However, the specific mechanisms employed by this medicinally important species to cope with high Al levels and the extent of Al accumulation in tissues remain unknown. Given that Al binds to phytoecdysteroids and cell wall components in root apices, it is of utmost importance to determine the effect of Al on the plant's redox metabolism and expression of genes involved in the production of various secondary metabolites. Understanding the translocation patterns of Al within *P. glomerata* is essential for developing strategies to control and reduce Al accumulation in this and other medicinal plants.

Given the hypothesis that *P. glomerata* mitigates aluminum toxicity through tissue-specific adjustments in redox metabolism, accumulation of protective metabolites, and regulation of genes related to cell wall structure and 20-E biosynthesis, this study aimed to determine whether *P. glomerata* tolerates Al stress by modulating redox metabolism, altering the expression of genes involved in cell wall composition, regulating 20-E biosynthesis, and exhibiting morphological changes under in vitro conditions.

Materials and methods

Plant material and in vitro cultivation

The experiment was carried out at the Plant Tissue Culture Laboratory (LCT) of the Institute of Biotechnology Applied to Agriculture (BIOAGRO), Federal University of Viçosa (UFV), Brazil. Authorization to access the genetic material was obtained from the Brazilian National System for the Management of Genetic Heritage and Associated Traditional

Knowledge (SISGEN, registration no. AA2A367), in compliance with current national biodiversity regulations.

The plant material used corresponded to the Alto do Caparaó accession, maintained in the in vitro germplasm bank of LCT-BIOAGRO. Cultures were subcultured every 30 days on MS basal medium with vitamins (Murashige and Skoog, 1962; Powder mixture No. M519, Phytotech Labs, Lenexa, Kansas), devoid of casein hydrolysate and plant growth regulators, and supplemented with 3.0% (w/v) sucrose. The medium was solidified with 0.55% (w/v) micropropagation-grade agar from Gelidium (Agar Plant TC, A296, Gel strength 910 g cm^{-2}, Phytotech Labs). Three nodal segments (~2 cm in length) from the Alto do Caparaó accession were inoculated into glass flasks containing 100 mL of liquid MS medium. The explants were supported on customized polypropylene holders, and the flasks were sealed with rigid polypropylene lids equipped with two 10-mm openings covered by 0.45-µm hydrophobic fluoropore membranes (MilliSeal® AVS-045; Air Vent, Tokyo, Japan), allowing CO_2 exchange at a rate of 25 µL L^{-1} s^{-1} (Batista et al. 2019). Cultures were maintained at 25 ± 2 °C under 60 µmol m^{-2} s^{-1} irradiance and a 16-h photoperiod for 40 days.

Aluminum stress was induced by supplementing the medium with five Al concentrations: 0, 200, 400, 600, and 800 µM (Sigma-Aldrich Co.). Aluminum solutions (supplied as $AlCl_3 \cdot 6H_2O$, pH 4.5) were sterilized by filtration under laminar airflow (Millipore® filters, Sigma-Aldrich) and added to the culture medium previously autoclaved at 1.5 atm and 120 °C for 20 min. The medium pH of all treatments was adjusted to 4.5 before inoculation. Cultures were maintained in a controlled-environment growth room at 25 ± 2 °C, 60 µmol m^{-2} s^{-1} irradiance provided by two SMD 100 LED lamps (18 W; Vilux, Vitória, ES, Brazil), and a 16-h photoperiod.

The experimental design was completely randomized, with five treatments (0, 200, 400, 600, and 800 µM Al), each comprising 20 replicates. Each experimental unit consisted of one flask containing three explants, and the total cultivation period was 40 days.

Growth parameters

The following variables were evaluated: root, stem, and leaf dry mass (g); total shoot length (cm) (measured from the root collar to the tip of the taproot); root length (cm); leaf area (cm^2); and number of leaves. Leaf area was quantified from digital images using ImageJ software. Root morphological traits were analyzed with the WinRhizo Pro system (Régent Instruments, Quebec, QC, Canada), which provided measurements of total root length (cm), surface area (cm^2), average diameter (cm), and volume (cm^3).

In vitro photosynthetic rate

Gas exchange and in vitro photosynthetic rates were measured following Costa et al. (2014), with modifications by Silva et al. (2020), using an AQ-S151 infrared CO_2 analyzer (Qubit Systems). Reference CO_2 was obtained by channeling ambient air into an empty flask at 300 mL min^{-1} under red and blue LED lighting (600 µmol m^{-2} s^{-1}). Plants were dark-adapted for 8 h before analysis. CO_2 levels were then recorded with plant-containing flasks, and gas exchange was calculated as the difference from the reference value. Air temperature and humidity were monitored using a Spec sensor (Thermo Recorder RS-11). More details of this methodology are available at Online Resource 1 (Supplementary Methods).

Anatomical characterization

After 40 days of cultivation in induction medium, the third pair of fully expanded leaves and root apices were collected and fixed in 4% glutaraldehyde (Karnovsky 1965). The fixed tissues were dehydrated through a graded ethanol series, embedded in methacrylate resin (Historesin; Leica, Wetzlar, Germany), and placed in plastic histomolds (Leica). Transverse sections of 5 µm thickness were obtained using an automatic-feed rotary microtome (RM2155; Leica) and stained with toluidine blue (pH 3.2) for 3 min (O'Brien and McCully 1981). The sections were mounted on glass slides with Permount mounting medium (Fisher Scientific, Waltham, MA, USA). Images were captured using a light microscope (AX70 TRF; Olympus Optical, Tokyo, Japan) equipped with a U-photo system and a digital color camera (Spot Insight 3.2.0) controlled by Spot Basic software (Diagnostic Instruments Inc., Sterling Heights, MI, USA).

Aluminum quantification

Al concentration was determined using 0.5 g of leaf and root tissues, dehydrated at 50 °C for 72 h, and ground in a knife mill to particles smaller than 1 mm. The extracts were obtained by digestion in a nitroperchloric solution (Malavolta et al. 1997), and Al content was determined using an inductively coupled plasma atomic emission spectrometer (Optima 7300 DV; PerkinElmer Inc., Shelton, CT, USA). Values were expressed in mg kg^{-1} of dry matter.

Carbohydrates, amino acids, and protein quantification

Leaf and root samples (~10 mg) were extracted with methanol following Lisec et al. (2006). Samples were frozen in liquid nitrogen, ground, lyophilized, and incubated with

methanol at 80 °C for 20 min. After centrifugation, supernatants were used to quantify photosynthetic pigments, sugars, and amino acids. Sugars were determined enzymatically using a 96-well microplate assay with sequential enzyme additions and absorbance readings at 340 nm. Amino acids were quantified using the ninhydrin reagent, with absorbance measured at 570 nm. The remaining precipitate was used to determine starch and protein contents. Protein was quantified by the Bradford method (595 nm), and starch by enzymatic hydrolysis followed by spectrophotometric analysis at 340 nm. Calculations were based on standard curves and the Lambert-Beer equation. More details of this methodology are available at Online Resource 1 (Supplementary Methods).

Photosynthetic pigments determination

To quantify photosynthetic pigments, 25 µL methanolic extract (see above) was combined with 175 µL methanol in 96-well microplates. Absorbance readings were obtained using a microplate reader (OptiMax; Molecular Devices, San Jose, CA, USA) at 470 nm (carotenoids), 666 nm (chlorophyll *a*), and 653 nm (chlorophyll *b*). Calculations were performed using the equations described by Wellburn (1994).

Proline content

Proline content was determined as described by Bates et al. (1973). In a microplate, 50 µL methanolic extract was mixed with 100 µL acidic ninhydrin solution [1% (w/v) ninhydrin in 60% (v/v) acetic acid and 20% (v/v) ethanol]. The microplate was sealed with Al tape and incubated at 95 °C for 20 min. Absorbance was measured at 520 nm, and a calibration curve was prepared using a standard proline solution (Sigma-Aldrich).

Quantification of oxidative stress enzymes

Catalase, APX, SOD, and POD activities were measured from leaf and root extracts (50 mg tissue homogenized in phosphate buffer containing EDTA, PMSF, and PVP). After centrifugation, the supernatant was used for enzymatic assays in microplates. CAT, APX, and POD activities were monitored by changes in absorbance at 240, 290, and 470 nm, respectively, and expressed as µmol min^{-1} mg^{-1} protein. SOD activity was based on inhibition of nitro blue tetrazolium photoreduction under light and expressed as U min^{-1} mg^{-1} protein. More details of this methodology are available at Online Resource 1 (Supplementary Methods).

Determination of lipid peroxidation levels

Lipid peroxidation was determined by quantifying MDA levels as proposed by Heath and Packer (1968), with modifications. Briefly, 1 mL of 1% trichloroacetic acid was added to 100 mg fresh macerated plant material. The solution was stirred in a vortex and centrifuged at 12,000 × *g* for and 4 °C for 15 min. Then, 250 µL supernatant was transferred to new tubes containing 750 µL of 0.5% 2-thiobarbituric acid (w/v) in 20% (w/v) trichloroacetic acid. The tubes were incubated with shaking at 95 °C and stopped in an ice bath for 30 min. The supernatants were transferred to new tubes, centrifuged (10,000 × *g* and 4 °C for 10 min), and absorbance was read at 532 (A_{532}) and 600 (A_{600}) nm. The MDA concentration was determined by subtracting A600 from A532 and calculated using an extinction coefficient of 155 mM cm^{-1}.

Expression analysis using qRT-PCR

The levels of *PgPhantom* (Cyp306a1), *PgSpook* (Cyp307a1), *PgC4H*, *PgCCoAOMT*, *PgCCR*, and *PgCAD* were determined. The leaves or roots (100 mg) were collected in liquid nitrogen, macerated, and subjected to total RNA extraction using TRI Reagent® (Sigma-Aldrich). The material was treated with DNAse I (Thermo Scientific NanoDrop Technology, Wilmington, DE, USA) to remove possible contamination with genomic DNA, and around 500 ng of extracted total RNA was converted to cDNA using the SuperScript™ III First-Strand Synthesis System (Invitrogen, Carlsbad, CA, USA). qRT-PCR was performed on a CFX96 Touch™ thermocycler (Bio-Rad Laboratories, Hercules, CA, USA) using specific primers from the *P. glomerata* transcriptome and *PgGAPDH* as internal reference (Batista et al. 2019).

The reactions were performed in duplicate with three biological replicates. The reaction volume of 10 µL included 4 µL SYBR-Green, 1 µL (4 µM) of each primer, 3 µL diethylpyrocarbonate-treated water, and 1 µL (40 ng) cDNA. Amplification conditions were as follows: 2 min at 50 °C and 10 min at 95 °C, followed by 40 cycles at 95 °C for 16 s and 60 °C for 60 s, and a dissociation curve from 60 to 95 °C at 0.1 °C s^{-1}. Transcript levels were determined using the $2^{-\Delta\Delta Ct}$ method (Livak and Schmittgen 2001), with three biological replicates and at least two technical replicates each. Primer sequences are listed in Supplementary Table S1. The melting curves were checked for nonspecific amplification and primer dimerization.

Data analysis

All the experiments were conducted using a completely randomized design with four biological replicates composed by a flask with three plants, per treatment. When replications

techniques existed, these were averaged as a single plot. Each experiment was repeated twice independently. Data was first tested for homogeneity (Bartlett's test) and normality (Shapiro-Wilk's test) and subsequently subjected to analysis of variance at $p \leq 0.05$. Differences in the means ($p < 0.05$) presented in the figures were evaluated using Tukey's test. Gene expression data were compared using Dunnett's test. All statistical analyses were performed in R (http://www.r-project.org).

Results

Growth inhibition and aluminum accumulation in *P. glomerata* under Al stress

Al exerted distinct effects on the growth of roots and aerial parts of *P. glomerata* (Fig. 1). Concentrations ≤ 400 µM Al promoted shoot and root length elongation; whereas concentrations higher than 600 µM Al caused drastic shortening of root length (50%) and shoot length (20%) compared to the control (Fig. 1k, l). Root dry mass was negatively affected at all tested Al concentrations (200, 400, 600, and 800 µM), with reductions of 33, 16, 34, and 50%, respectively (Fig. 1m). A similar trend was observed for shoot dry mass, which dropped by 30% (600 µM Al) and 45% (800 µM Al) (Fig. 1n). Leaf area was also negatively affected, decreasing by 27% (600 µM Al) and 17% (800 µM Al) (Fig. 1o). In contrast, no change was observed with respect to leaf number (Fig. 1p). A significant decrease in root diameter (18%) was observed only at 400 µM Al (Fig. 1q); while total root length became shorter by 35, 47, 41, and 55% at 200, 400, 600, and 800 µM, respectively (Fig. 1r). Root volume was negatively affected (−35%) only at the highest Al concentration tested (800 µM) (Fig. 1s). After Al exposure, *P. glomerata* accumulated Al in both roots and leaves. Root Al levels increased by 140% to 1900%, and leaf levels by 46% to 81%, depending on the Al concentration (200–800 µM), compared to controls. (Online Resource 1, Supplementary Fig. S1).

Aluminum induces morphoanatomical changes in *P. glomerata*

Morphological changes were observed in the leaves of plants exposed to Al (Fig. 2). Control leaves displayed a uniseriate epidermis, a prominent central vascular bundle with parenchyma distributed along the main vein, and collenchyma subdivided into palisade and spongy parenchyma (Fig. 2a). In contrast, Al-treated plants exhibited enlarged parenchyma cells, a disorganized vascular bundle, irregularly shaped palisade parenchyma cells, and loss of intercellular spaces in the spongy parenchyma at increasing Al concentrations (Fig. 2h, k, n). In the roots, Al exposure altered cortical thickness (Fig. 2f, i, o). Finally, the xylem was more developed at higher Al concentrations (Fig. 2i, l, o). There were no significant variations in photosynthetic pigments and photosynthetic rate with plant exposure to Al (Online Resource 1, Supplementary Fig. S2).

Aluminum induces metabolic alterations in *P. glomerata*

Aluminum exposure triggered pronounced changes in the primary metabolism of *P. glomerata* (Fig. 3). Glucose and fructose increased substantially to 600 µM Al (120%) and 800 µM Al (160%) (Fig. 3a, b). Fructose content followed a consistent trend, with increases of 46 and 63% at 600 and 800 µM Al, respectively, compared to the control (Fig. 3b). Sucrose content also showed an increasing trend with rising Al concentrations, augmenting by 38% at 800 µM Al (Fig. 3c). Similarly, starch content rose by 60 and 28% at 600 and 800 µM Al, respectively (Fig. 3d).

Total amino acid content increased significantly (74%) to only 600 µM Al, while other concentrations did not differ from the control (Fig. 3e). No consistent pattern was observed for total protein content (Fig. 3f). Among stress-related metabolites, total phenolic content increased by 16 and 8% at 600 and 800 µM Al, respectively (Fig. 3g). Proline content increased by an average of 90% across all tested concentrations (Fig. 3h). Malate content increased in response to all Al concentrations, with the most pronounced accumulation (100% increase) observed at 600 µM Al (Fig. 3i). Fumarate levels also tended to increase with Al exposure, although a significant increase (56%) was detected only at 600 µM (Fig. 3j).

Aluminum influences antioxidant enzyme activity and lipid peroxidation in *P. glomerata*

Activity of the antioxidant enzymes catalase, peroxidase oxidoreductase (POD), and superoxide dismutase (SOD) was significantly affected by the presence of Al (Fig. 4). Compared to the control, 200, 600, and 800 µM Al boosted catalase activity by 32, 17, and 20%, respectively (Fig. 4a, b). POD activity increased significantly in both leaves and roots at all Al concentrations tested, although the greatest effect was observed at 600 µM (Fig. 4c, d). SOD activity increased at all Al concentrations tested, particularly in the roots (Fig. 4e, f). Increases of 34, 37, 29, and 46% were recorded at 200, 400, 600, and 800 µM Al, respectively (Fig. 4f). Whereas malondialdehyde (MDA) levels decreased significantly in the leaves (Fig. 4g); they rose by 15, 23, 43, and 27% at 200, 400, 600, and 800 µM Al, respectively, in

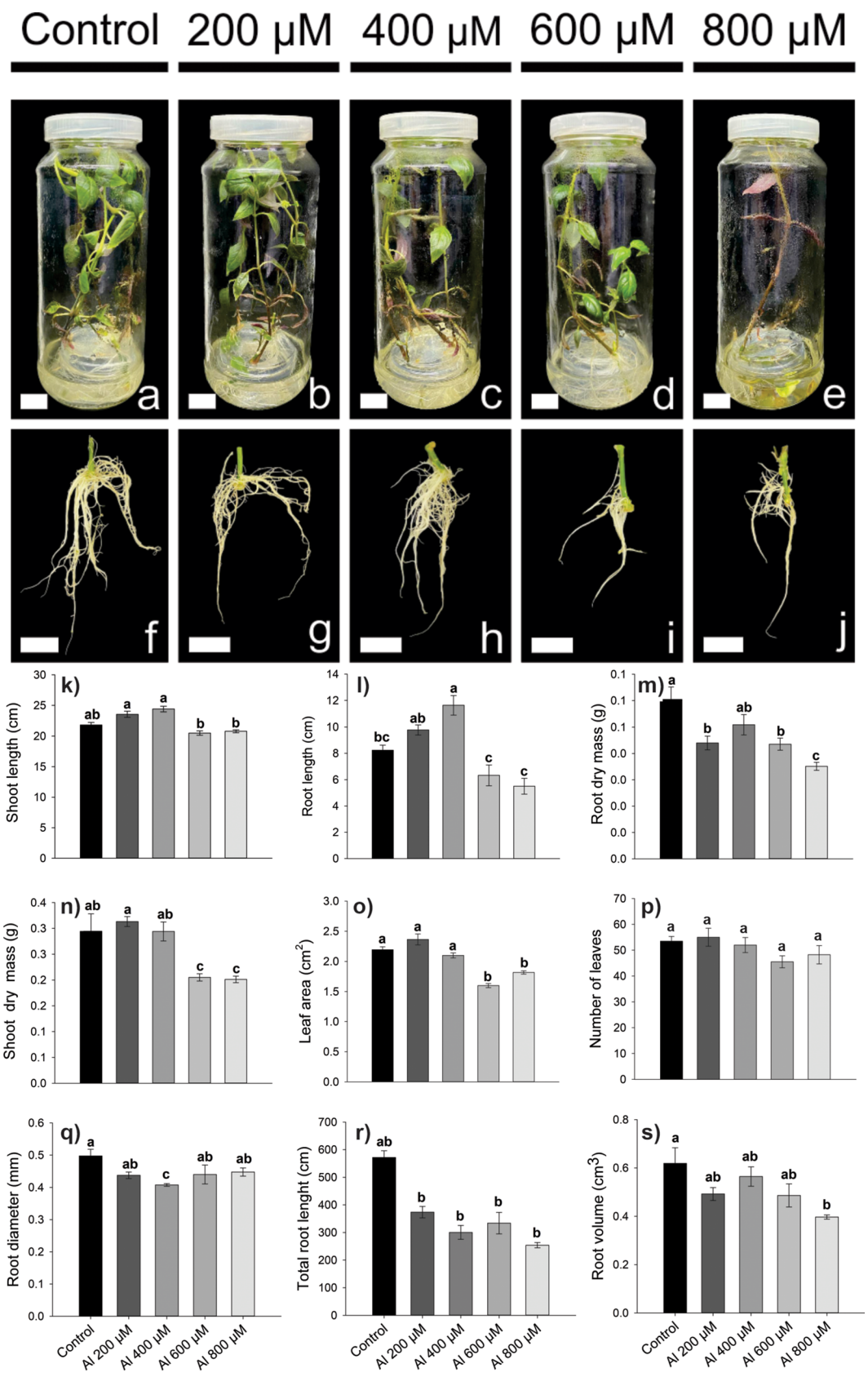

Control
200 µM
400 µM
600 µM
800 µM
a
b
c
d
e
f
g
h
i
j
k)
Shoot length (cm)
l)
Root length (cm)
m)
Root dry mass (g)
n)
Shoot dry mass (g)
o)
Leaf area (cm²)
p)
Number of leaves
q)
Root diameter (mm)
r)
Total root lenght (cm)
s)
Root volume (cm³)
Control
Al 200 µM
Al 400 µM
Al 600 µM
Al 800 µM

Fig. 1 Growth aspects of *P. glomerata* after 40 days of in vitro cultivation under the following conditions: (**a, f**) Control; (**b, g**) 200 µM Al; (**c, h**) 400 µM Al; (**d, i**) 600 µM Al; and (**e, j**) 800 µM Al. (**k**) shoot length; (**l**) root length; (**m**) root dry mass; (**n**) shoot dry mass; (**o**) leaf area (cm^2); (**p**) leaf number; (**q**) root diameter; (**r**) total root length; and (**r**) root volume. Values are presented as means ± standard error ($n = 4$). Means followed by the same letters did not differ according to Tukey's test ($p \leq 0.05$). Scale bars: 30 mm

the roots (Fig. 4h). This dichotomy suggested differential oxidative stress responses between the two organs.

Aluminum modulates the expression of genes related to the lignin and 20-E biosynthetic pathways

In the leaves, the cinnamoyl-CoA reductase (*PgCCR*) gene related to lignin production via the phenylpropanoid biosynthesis pathway was upregulated only at 800 µM Al (Fig. 5a). Conversely, in the roots, it was downregulated by 0.4, 0.6, 0.6, and 0.8 times at 200, 400, 600, and 800 µM Al, respectively (Fig. 5b). Expression of the cinnamyl alcohol dehydrogenase (*PgCAD*) gene was upregulated in the leaves at all Al doses (Fig. 5c) but slightly downregulated at 800 µM Al (Fig. 5d).

The cinnamate 4-hydrogenase (*PgC4H*) gene in the leaves showed a 0.5- to 1.3-fold increase at increasing Al concentrations, compared to the control (Fig. 5e). In contrast, in the roots, *PgC4H* decreased by 0.4- and 0.7-fold at 600 and 800 µM Al, respectively, compared to the control (Fig. 5f). Expression of the caffeoyl-CoA O-methyltransferase (*PgCCoAOMT*) gene did not differ significantly in the leaves (Fig. 5g) but was reduced by 0.8- to 0.6-fold in the roots in the presence of Al (Fig. 5h).

Expression of the cytochrome P450 family subfamily A (*PgSpook*) and ecdysteroid 25-hydroxylase (*PgPhantom*) genes involved in 20-E biosynthesis was differentially affected by Al toxicity. *PgSpook* in the leaves was not affected by Al (Fig. 5i) but declined by 3-fold in the roots of *P. glomerata* at 200 µM Al and followed a similar trend at all concentrations tested (Fig. 5j). *PgPhantom* was downregulated in the leaves and roots in response to Al toxicity (Fig. 5k, l).

Discussion

In this study, we investigated the effect of Al toxicity on the morphophysiological and molecular responses of in vitro-grown *P. glomerata*. The most evident symptoms of Al toxicity observed in the aerial parts included the curling of young leaves, smaller leaf size, purpling of stems and leaves, yellowing and necrosis of leaf tips, and general chlorosis and tissue death. Exposure to concentrations higher than 600 µM Al significantly inhibited root and shoot development, reducing total plant biomass. These findings are consistent with those of Maldaner et al. (2015), who reported similarly lower root and shoot growth in two *P. glomerata* accessions under Al stress. The observed growth impairments are likely due to Al-induced disruption of key physiological processes, including nutrient absorption and transport, leading to nutrient imbalances (Umar et al. 2025).

Root growth inhibition is a hallmark of Al toxicity and is largely attributed to fewer cell divisions within the root apical meristem (Ur Rahman et al. 2024; Huang and Ma 2025). Al exposure blocks mitotic activity, alters microtubule organization, and disrupts cytoskeletal integrity, all of which impede normal cell division and elongation (Boniotti 2002). However, the severity of Al toxicity varies widely across plant species, depending on developmental stage, growth conditions, Al concentration, and exposure duration.

Here, concentrations higher than 600 µM Al markedly reduced growth and leaf size of *P. glomerata* plants. Interestingly, no changes were observed in leaf number, demonstrating that the photosynthetically active area was preserved to a sufficient degree to sustain gas exchange and photosynthesis under moderate stress conditions. This suggests the presence of compensatory mechanisms, such as increased cell division or adjustments in chloroplast density, that maintain photosynthetic efficiency under abiotic stress (Ferjani et al. 2007; Jiang et al. 2012). Consistent with these observations, total root length was reduced by at least 30% at all Al concentrations tested, along with decreased root diameter, reduced elongation, and cellular deformation, which collectively impaired root hair development and damaged root apices. These responses match previous reports of Al-induced structural damage and compromised root functionality (Panda et al. 2009; Engel et al. 2021).

The concentration of Al in *P. glomerata* leaves increased proportionally with Al availability in the medium, exhibiting a linear accumulation pattern. We speculate that Al^{3+} ions reached the vascular tissues primarily via symplastic transport, whereby membrane crossing was coupled to energy expenditure and hydrogen ion (H^+) influx (Ur Rahman et al. 2024). The latter may contribute to alkalinization of the rhizosphere or growth medium, thereby mitigating Al toxicity in the roots and representing a potential adaptive response to Al-contaminated soils.

Intracellular Al detoxification in plants is often associated with complexation by organic acids such as malate, oxalate, and citrate, which can reduce the availability of free Al^{3+} in the cytosol and facilitate its compartmentalization (Sade et al. 2016; Gupta et al. 2013; Nunes-Nesi et al. 2007, Sami et al. 2020). These processes have been linked in other systems to the activity of plasma membrane and vacuolar transporters that contribute to cytosolic homeostasis and stress tolerance. In the present study, the accumulation of Al

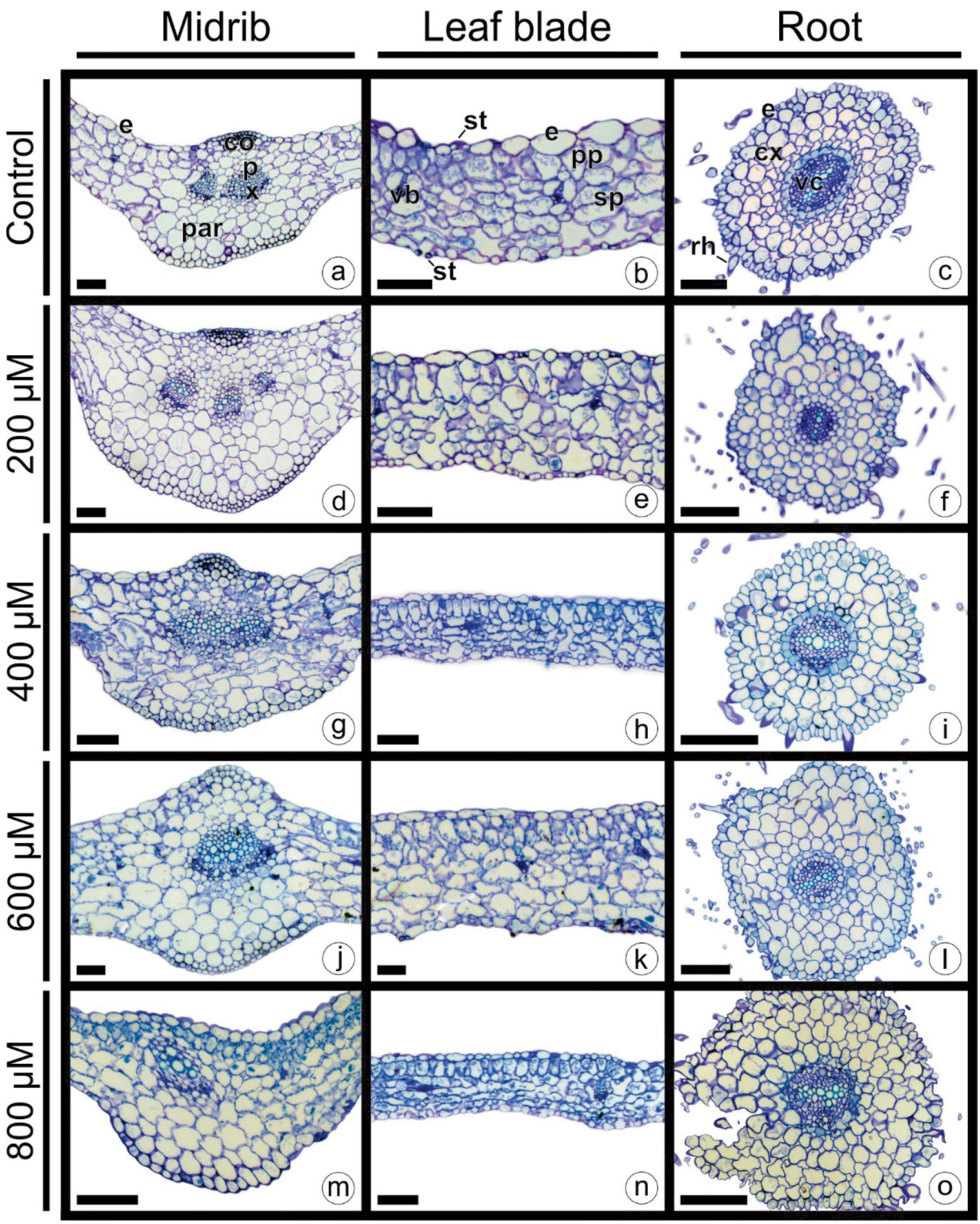


Fig. 2 Anatomical characterization of leaves (midrib and leaf blade) and roots in cross-sections of *P. glomerata* plants after 40 days of in vitro cultivation with 0, 200, 400, 600, and 800 µM Al. Abbreviations: *e* – epidermis; *co* – collenchyma; *fc* – fascicular cambium; *ic* – interfascicular cambium; *par* – parenchyma; *p* – phloem; *pp* – palisade parenchyma; *sp* – spongy parenchyma; *st* – stomata; *sx* – secondary xylem; *vb* – vascular bundle; *x* – xylem. Scale bars: 100 µm

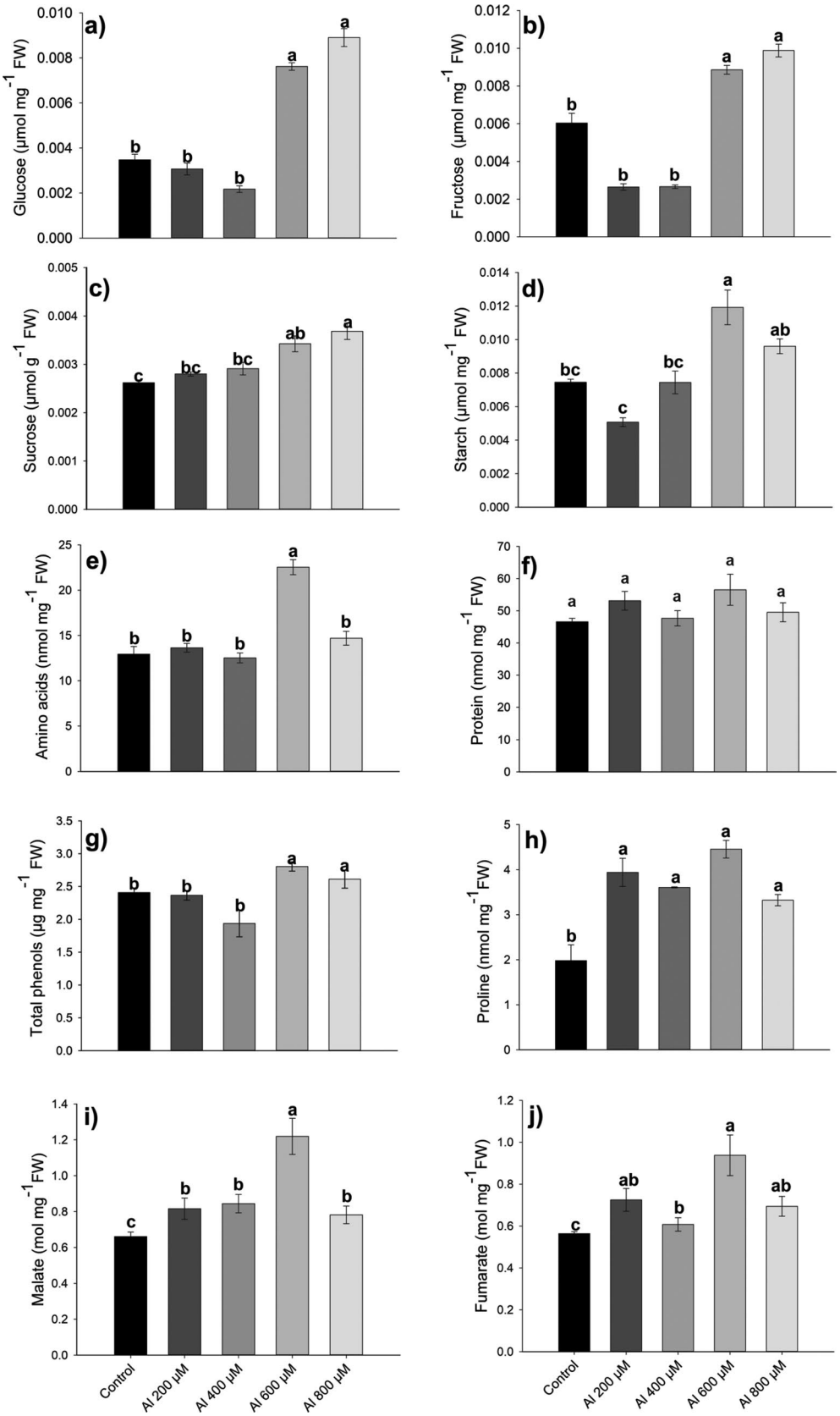


Fig. 3 Changes in the primary metabolism of *P. glomerata* after 40 days of in vitro cultivation with 0, 200, 400, 600, and 800 µM Al. (**a**) Glucose; (**b**) fructose; (**c**) sucrose; (**d**) starch; (**e**) total proteins; (**f**) total amino acids; (**g**) total phenols; and (**h**) proline. Values are presented as means ± standard error ($n = 6$). Means followed by the same letters did not differ according to Tukey's test ($p \leq 0.05$)

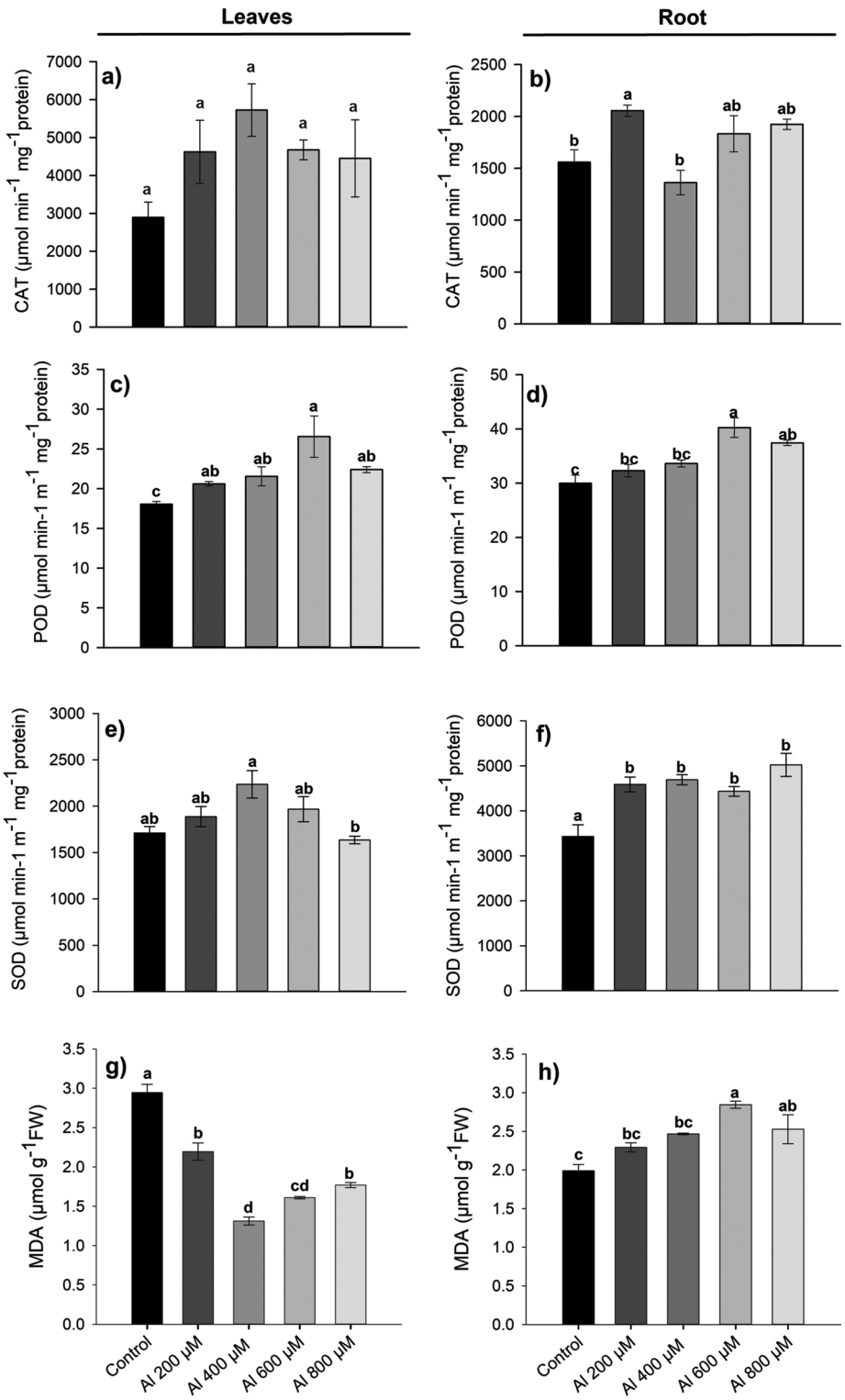


Fig. 4 Antioxidant enzyme activity in *P. glomerata* after 40 days of in vitro cultivation with 0, 200, 400, 600, and 800 µM Al. (**a**) Catalase (leaves); (**b**) catalase (roots); (**c**) POD (leaves); (**d**) POD (roots); (**e**) SOD (leaves); (**f**) SOD (roots); (**g**) MDA content (leaves); and (**h**) MDA content (roots). Values are presented as means ± standard error ($n = 6$). Means followed by the same letters did not differ according to Tukey's test ($p \leq 0.05$)

in roots and leaves, together with increased levels of malate and fumarate at 600 µM Al, suggests the possible involvement of organic acid–mediated detoxification mechanisms. However, direct evidence for vacuolar sequestration, transporter activity, or Al–organic acid complex formation was not assessed here, and these interpretations should therefore be viewed as putative. Further studies integrating root exudation, subcellular fractionation, and transporter analyses will be necessary to confirm these mechanisms in *P. glomerata*.Plant growth under stressful conditions is often accompanied by altered carbon metabolism. Here, plants exposed to concentrations higher than 600 µM Al accumulated

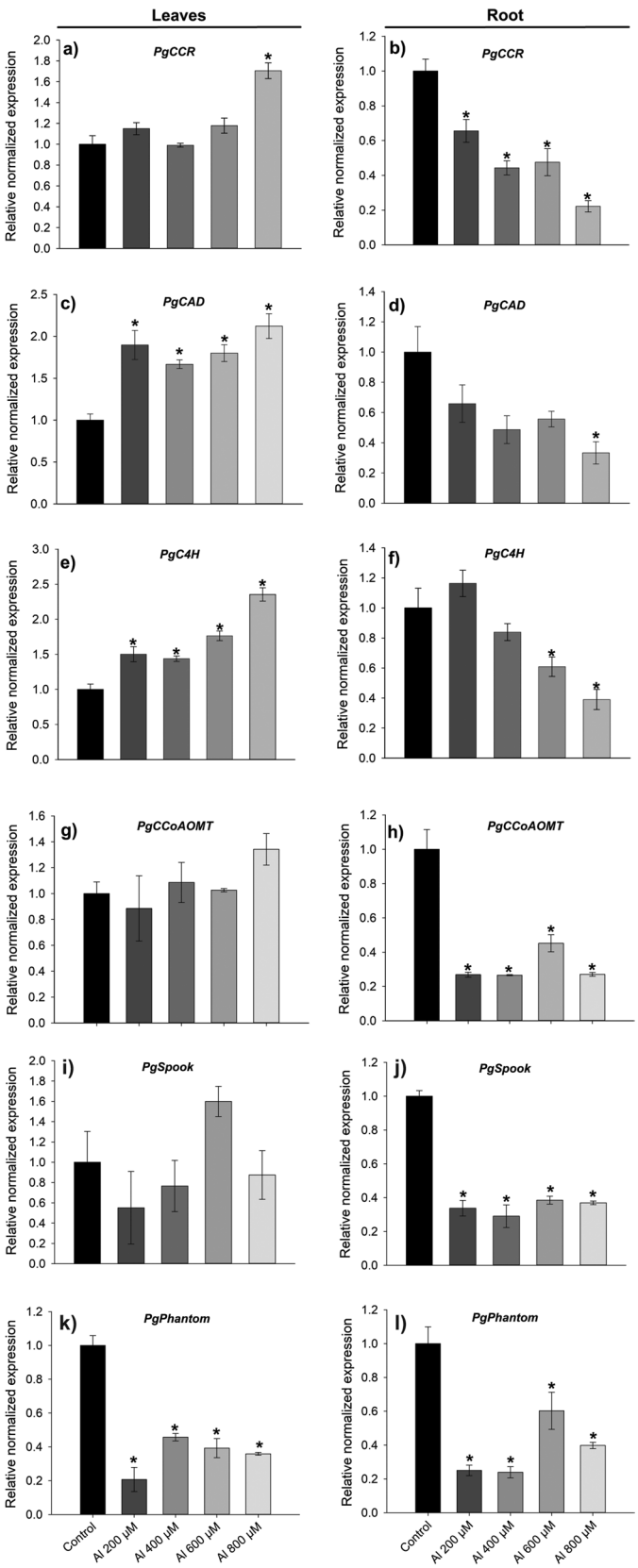


Fig. 5 Relative expression of lignin and 20-hydroxyecdysone synthesis pathways genes in *P. glomerata* plants grown in vitro for 40 days with 0, 200, 400, 600, and 800 µM Al. (**a**) *PgCCR* (leaves); (**b**) *PgCCR* (roots); (**c**) *PgCAD* (leaves); (**d**) *PgCAD* (roots); (**e**) *PgC4H* (leaves); (**f**) *PgC4H* (roots); (**g**) *PgCcoaomt* (leaves); (**h**) *PgCcoaomt* (roots); (**i**) *PgSpook* (leaves); (**j**) *PgSpook* (roots); (**k**) *PgPhantom* (leaves); and (**l**) *PgPhantom* (roots). Expression was normalized to *PgGAPDH*. Values are presented as means ± standard error ($n = 3$). Asterisks indicate a significant difference by Dunnett's test ($p \leq 0.05$)

high levels of glucose and fructose, and, to a lesser extent, sucrose. These sugars likely serve as osmoprotectants and energy reserves that support cellular metabolism and survival under Al-induced stress (De La Mata et al. 2013). Proline is involved in protein synthesis and plant development (Spormann et al. 2021), as well as in stress mitigation, by serving as a compatible solute, ROS scavenger, and molecular chaperone that stabilizes proteins and membranes. Changes in proline metabolism can affect the cellular redox state, triggering metabolic adjustments (Ghosh et al. 2021). We observed an increase in proline at all Al concentrations. Exposure to metals alters proline levels, suggesting a protective effect against metal-induced damage. Our findings indicate that proline contributes to Al stress tolerance by mitigating oxidative damage, maintaining cytosolic pH, and possibly acting as a source of energy, carbon, and nitrogen during post-stress recovery (Szabados and Savouré 2010; Sousa et al. 2020; Fortini et al. 2023).

In addition to organic acid-mediated detoxification, morphological changes, and stress-related gene expression, antioxidant defense mechanisms are crucial for coping with Al-induced oxidative stress. In *P. glomerata*, Al exposure stimulated the activity of key ROS-scavenging enzymes, including catalase, POD, and SOD. However, increased lipid peroxidation, as indicated by higher MDA content, was observed in the roots across all Al concentrations, suggesting persistent oxidative stress (Fig. 4g, h). These results are consistent with those of Bernardy et al. (2020), who reported elevated MDA levels in *P. glomerata* roots under Zn stress. Activation of antioxidant systems likely prevents excessive ROS accumulation, thereby protecting cellular membranes, proteins, and DNA from oxidative damage, which could otherwise trigger programmed cell death (Sami et al. 2020).

The interaction of Al with cell wall and symplastic components, especially in the root apices, disturbs the homeostasis and promotes ROS production. This is primarily due to the high reactivity of Al^{3+}, which enables it to bind to epidermal and cortical cells, the plasma membrane, the cell wall matrix, the nucleus, and cytoskeletal elements (Panda et al. 2009; Manquián-Cerda et al. 2018). For example, the interaction of Al ions with the plasma membrane of roots stimulates callose production, restricting cell-to-cell transport and disrupting the redox balance (Sun et al. 2020). In our study, this was supported by the significant increase in POD and SOD activities, especially in the roots. Enzymatic antioxidant systems play an important role in reducing oxidative damage to cellular components (Kesawat et al. 2023). In addition, Al interferes with the proper functioning of the plasma membrane by interacting with lipids and causing lipid peroxidation (Kochian et al. 2015). Hydrogen peroxide (H_2O_2), hydroxyl radicals (•OH), and singlet oxygen ($^1O_2$) are generated primarily in the mitochondria, chloroplasts, and peroxisomes. These ROS not only contribute to oxidative stress, but may also function as signaling molecules, regulating the expression of ROS-scavenging enzymes and activating protective metabolic pathways (Guo et al. 2023). Although not evaluated here, it has been demonstrated that phytohormone signaling and cross-talk can also participate in regulating plant responses to Al toxicity, further modulating protective mechanisms against stress (Ranjan et al. 2021).

Al promotes differential gene expression involved in the modulation of phytoecdysteroid biosynthesis. *De novo* assembly of the *P. glomerata* transcriptome revealed several genes in the CYP P450 family related to secondary metabolism and stress (Batista et al. 2019). Here, we evaluated the relative expression of *PgSpook* and *PgPhantom*, two family members involved in 20-E biosynthesis under abiotic stress (Batista et al. 2019). Interestingly, *PgSpook* (CYP83A) was negatively regulated at all levels of Al exposure, mainly in the roots. Similarly, *PgPhantom* (CYP76C) was strongly downregulated in both roots (up to a 10-fold decrease) and leaves (a 5-fold decrease). These results suggested that Al suppressed the transcription of genes involved in 20-E biosynthesis and contrasted with those of Felipe et al. (2019), who showed that salt stress and ultraviolet B radiation upregulated *PgSpook* and *PgPhantom*. Hence, the regulation of 20-E biosynthesis genes may be stress-specific. Furthermore, in *Panax ginseng*, interactions of heavy metals with the cell membrane upregulate several defense-related genes via the jasmonic acid pathway (Balusamy et al. 2013). Although studies addressing aluminum tolerance in medicinal plant species remain scarce, evidence from non-accumulator species indicates that organic acid anions within root tissues play an important role in Al detoxification, as demonstrated in the *Brachiaria* hybrid (Watanabe et al. 2006), highlighting potentially conserved mechanisms that may also operate in medicinal plants.

A similar modulatory pattern was observed in genes involved in the phenylpropanoid metabolic network, which also belongs to the multigenic CYT family (CYP73, CYP98, and CYP84) (Renault et al. 2017; Hansen et al. 2021). Among these, we evaluated the expressions of *PgCCR*, *PgCAD*, *PgC4H*, and *PgCCoAOMT*, which are involved in the synthesis of lignin and its fractions, suberin, and cutin. Al upregulated *PgCCR* in the leaves only at the highest concentration tested, while downregulating it in the roots, where it binds strongly to cell walls. There, the Al^{3+} ion might saturate all active sites, which may alter the integrity, coupling, and polymerization of microtubules and the cytoskeleton. We observed a significant increase in Al-mediated *PgC4H* expression in the leaves and a negative increase in the roots. Al downregulated *PgCCoAOMT* in *P. glomerata* roots, but

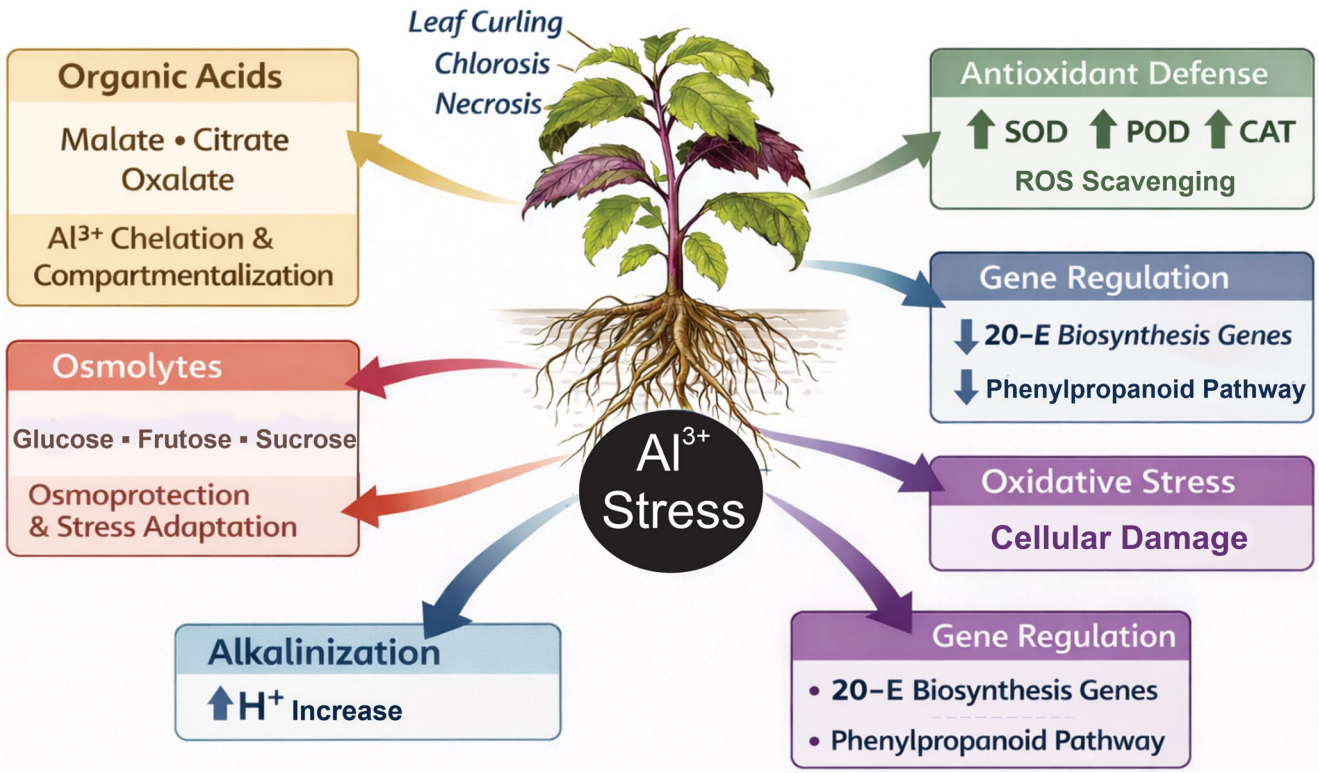


Fig. 6 Aluminum tolerance mechanisms in *Pfaffia glomerata*. The schematic illustrates Al stress perceived primarily at the root system and the main physiological and metabolic adjustments associated with tolerance, including osmolyte accumulation (e.g., sugars), modulation of organic acids, and rhizosphere/cellular alkalization. Boxes summarize the key response in leaves and roots, providing an integrated, simplified view of mechanisms underlying Al tolerance in this species

not in the leaves. This enzyme catalyzes the methylation of caffeoyl-CoA, which is a key step in lignin biosynthesis, using S-adenosylmethionine as a methyl donor (Weng et al. 2010). Suppression of *PgCCoAOMT* in the roots may result in reduced lignin deposition, compromising root structural integrity under stress.

This study provides novel insights into the Al stress responses of *P. glomerata*, revealing tissue-specific adaptations involving antioxidant defense, osmolyte accumulation, organic acid detoxification, and transcriptional regulation of phenylpropanoid and phytoecdysteroid pathways. Collectively, our results also suggest that *P. glomerata* is an Al-tolerant species, capable of maintaining physiological and metabolic functionality under Al-associated stress conditions. These integrated physiological and metabolic adjustments are summarized schematically in Fig. 6. Notably, we report for the first time the modulation of 20-E biosynthetic genes under Al stress, highlighting potential molecular targets for improving stress tolerance in medicinal and crop species. Although nutrient content was not assessed here due to scope and methodological constraints, future studies addressing nutrient uptake and transport under Al stress will be important to further elucidate the mechanisms underlying tolerance in this species. In addition, validation of these responses under soil or hydroponic conditions will be valuable for strengthening ecological and agronomic relevance. Finally, the practical implications of these findings warrant further discussion, particularly in the context of the potential industrial exploitation and large-scale production of *P. glomerata*–derived bioactive compounds.

Conclusions

P. glomerata exhibits a complex, tissue-specific response to aluminum toxicity, particularly at concentrations above 600 µM. Al exposure significantly impaired root and shoot growth, disrupted anatomical organization, and altered photosynthetic pigment content and carbon metabolism. The accumulation of osmoprotective metabolites, such as sugars, starch, malate, and fumarate accompanied these physiological changes. At the molecular level, Al modulated the expression of genes related to both structural integrity (e.g., *PgCCR*, *PgC4H*, *PgCCoAOMT*) and defense-related secondary metabolism, including phytoecdysteroid biosynthesis (*PgSpook* and *PgPhantom*), highlighting a coordinated reprogramming of stress-response pathways. Notably, this is the first report linking Al stress to the downregulation

of 20-hydroxyecdysone biosynthetic genes in a medicinal species, offering novel insights into the hormonal and metabolic adjustments involved in abiotic stress tolerance. However, the study is limited by its in vitro design, which may not fully replicate soil–plant interactions or long-term adaptation mechanisms. Future research should include in vivo experiments, time-course analyses, and analysis of potential genes involved in Al detoxification and tolerance. Overall, our findings expand current knowledge of Al stress responses in non-model plants and lay the groundwork for developing stress-resilient medicinal and crop species through metabolic and genetic approaches. The originality of this work lies in its integrative analysis of anatomical, physiological, metabolic, and transcriptional responses to Al, revealing potential targets for biotechnological or agronomic applications.

Supplementary Information The online version contains supplementary material available athttps://doi.org/10.1007/s11240-026-03346-w.

Acknowledgements Departamento de Biologia Vegetal (DBV/UFV), Departamento de Bioquímica e Biologia Molecular (DBB/UFV), Instituto de Biotecnologia Aplicada à Agropecuária (Bioagro/UFV), and Unidade de Crescimento de Plantas (UCP/UFV) are acknowledged for providing the necessary infrastructure. Editage (https://www.editage.com.br/) is acknowledged for the English editing.

Author Contribution MMVA and WCO designed and carried out the experiments and collected the data. MMVA, TDS, QPD, LEGM, MDHS, and ESS performed biochemical analyses. MMVA, AOM, MMVA, SHSF, DSB, EAF, JM, JMH, DSB, WLA, and WCO analyzed the data and wrote the manuscript.

Funding The Article Processing Charge (APC) for the publication of this research was funded by the Coordenação de Aperfeiçoamento de Pessoal de Nível Superior - Brasil (CAPES) (ROR identifier: 00x0ma614). This work was supported by the Fundação de Amparo à Pesquisa do Estado de Minas Gerais—FAPEMIG (grant numbers APQ-02372-17, APQ-00772-19, APQ-01433-22 and Rede Mineira Estresse em Plantas RED-00060-23), the Conselho Nacional de Pesquisa e Desenvolvimento Científico e Tecnológico—CNPq (grant number 406455/2022-8/INCT - Fisiologia do Estresse), and Coordenação de Aperfeiçoamento de Pessoal de Nível Superior—CAPES (Financial Code 0001). The following authors received scholarships from CNPq: MMVA (PDJ-153111-24). The research fellowships granted by the CNPq to WLA and WCO (grant number 310937/2022-1) are gratefully acknowledged. The Article Processing Charge for publishing this research was funded by the Coordination for the Improvement of Higher Education Personnel - CAPES (identifier ROR: 00x0ma614). For open access purposes, the authors have assigned the Creative Commons CC BY license to any accepted version of the article.

Data availability The authors confirm that the data supporting the findings of this study are available in the article.

Declarations

Ethical Approval Not applicable.

Competing interests W.C.O. serves as an Associate Editor of the journal at the time of submission. However, this did not influence the peer review process or the final decision. The remaining authors declare no conflicts of interest.

Open Access This article is licensed under a Creative Commons Attribution 4.0 International License, which permits use, sharing, adaptation, distribution and reproduction in any medium or format, as long as you give appropriate credit to the original author(s) and the source, provide a link to the Creative Commons licence, and indicate if changes were made. The images or other third party material in this article are included in the article's Creative Commons licence, unless indicated otherwise in a credit line to the material. If material is not included in the article's Creative Commons licence and your intended use is not permitted by statutory regulation or exceeds the permitted use, you will need to obtain permission directly from the copyright holder. To view a copy of this licence, visit http://creativecommons.org/licenses/by/4.0/.

References

MurashigeT,Skoog F (1962) A revised medium for rapid growth and bio assays with tobacco tissue cultures. Physiol Plant 15. https://doi.org/10.1111/j.1399-3054.1962.tb08052.x

Balusamy SRD, Kim Y-J, Rahimi S, Senthil KS, Lee OR, Lee S, Yang D-C (2013) Transcript pattern of cytochrome P450, antioxidant and ginsenoside biosynthetic pathway genes under heavy metal stress in *Panax ginseng* Meyer. Bull Environ Contam Toxicol 90:194–202. https://doi.org/10.1007/s00128-012-0891-5

Bates LS, Waldren RP, Teare ID (1973) Rapid determination of free proline for water-stress studies. Plant Soil 39:205–207. https://doi.org/10.1007/bf00018060

Batista DS, Koehler AD, Romanel E, Souza VC, Silva TD, Almeida MC et al (2019) *De novo* Assembly and transcriptome of *Pfaffia glomerata* uncovers the role of photoautotrophy and the P450 family genes in 20-hydroxyecdysone production. Protoplasma 256:601–614. https://doi.org/10.1007/s00709-018-1322-1

Bernardy K, Farias JG, Pereira AS et al (2020) Plants' genetic variation approach applied to zinc contamination: secondary metabolites and enzymes of the antioxidant system in *Pfaffia glomerata* accessions. Chemosphere 253:126692. https://doi.org/10.1016/j.chemosphere.2020.126692

Bojórquez-Quintal E, Escalante-Magaña C, Echevarría-Machado I, Martínez-Estévez M (2017) Aluminum, a friend or foe of higher plants in acid soils. Front Plant Sci 8. https://doi.org/10.3389/fpls.2017.01767

Boniotti MB (2002) "Cross-talk" between cell division cycle and development in plants. Plant Cell 14:11–16. https://doi.org/10.1105/tpc.140121

Calgaroto NS, Castro GY, Cargnelutti D et al (2010) Antioxidant system activation by mercury in *Pfaffia glomerata* plantlets. BioMetals 23:295–305. https://doi.org/10.1007/s10534-009-9287-3

Cárcamo MP, Reyes-Díaz M, Rengel Z et al (2019) Aluminum stress differentially affects physiological performance and metabolic compounds in cultivars of highbush blueberry. Sci Rep 9. https://doi.org/10.1038/s41598-019-47569-8

Chamier J, Wicht M, Cyster L, Ndindi NP (2015) Aluminum (al) fractionation and speciation; getting closer to describing the factors influencing Al3+ in water impacted by acid mine drainage. Chemosphere 130:17–23. https://doi.org/10.1016/j.chemosphere.2015.01.026

Chauhan DK, Yadav V, Vaculík M et al (2021) Aluminum toxicity and aluminum stress-induced physiological tolerance responses in

higher plants. Crit Rev Biotechnol 41:715–730. https://doi.org/10.1080/07388551.2021.1874282

Costa AC, Rosa M, Megguer CA et al (2014) A reliable methodology for assessing the in vitro photosynthetic competence of two Brazilian savanna species: *hyptis marrubioides* and *Hancornia speciosa*. Plant Cell Tiss Org Cult 117:443–454. https://doi.org/10.1007/s11240-014-0455-y

Cotrim-Ribeiro ST, Gancedo NC, Braz de Oliveira AJ, Correia Gonçalves RA (2024) A comprehensive review of *Pfaffia glomerata* botany, ethnopharmacology, phytochemistry, biological activities, and biotechnology. J Ethnopharmacol 328:118003. https://doi.org/10.1016/j.jep.2024.118003

Das N, Mishra SK, Bishayee A et al (2021) The phytochemical, biological, and medicinal attributes of phytoecdysteroids: an updated review. Acta Pharm Sin B 11:1740–1766. https://doi.org/10.1016/j.apsb.2020.10.012

De La Mata L, Cabello P, De La Haba P, Agüera (2013) Study of the senescence process in primary leaves of sunflower (*Helianthus annuus* L.) plants under two different light intensities. Photosynthetica 51:85–94. https://doi.org/10.1007/s11099-013-0001-x

Engel F, Cotelle S, Somensi CA et al (2021) A 3D ecotoxi-topological profile: using concentration-time-response surfaces to show peroxidase activity in *zea mays* (L.) exposed to aluminum or arsenic in hydroponic conditions. Chemosphere 262:127647. https://doi.org/10.1016/j.chemosphere.2020.127647

Farooq TH, Rafay M, Basit H et al (2022) Morpho-physiological growth performance and phytoremediation capabilities of selected xerophyte grass species toward Cr and Pb stress. Front Plant Sci 13. https://doi.org/10.3389/fpls.2022.997120

Felipe SHS, Batista DS, Vital CE, Chagas K, Silva PO, Silva TD, Fortini EA, Correia LNF, Ávila RT, Maldaner J, Festucci-Buselli RA, DaMatta FM, Otoni WC (2019) Salinity-induced modifications on growth, physiology and 20-hydroxyecdysone levels in Brazilian-ginseng [Pfaffia glomerata (Spreng.) Pedersen]. Plant Physiol Biochem 140:43–54. https://doi.org/10.1016/j.plaphy.2019.05.002

Ferjani A, Horiguchi G, Yano S, Tsukaya H (2007) Analysis of leaf development in *fugu* mutants of Arabidopsis reveals three compensation modes that modulate cell expansion in determinate organs. Plant Physiol 144:988–999. https://doi.org/10.1104/pp.107.099325

Fortini EA, Batista DS, Felipe SHS (2023) Physiological, epigenetic, and proteomic responses in *Pfaffia glomerata* growth in vitro under salt stress and 5-azacytidine. Protoplasma 260: 467–482. https://doi.org/10.1007/s00709-022-01789-4

Ghosh TK, Tompa NH, Rahman MM et al (2021) Acclimation of liverwort *marchantia polymorpha* to physiological drought reveals important roles of antioxidant enzymes, proline and abscisic acid in land plant adaptation to osmotic stress. PeerJ 9:e12419. https://doi.org/10.7717/peerj.12419

Gomes MP, Tcllsm M, Martins GA et al (2012) Cd-tolerance markers of *Pfaffia glomerata* (Spreng.) Pedersen plants: anatomical and physiological features. Braz J Plant Physiol 24:293–304. https://doi.org/10.1590/s1677-04202012000400008

Guo W, Xing Y, Luo X et al (2023) Reactive oxygen species: a crosslink between plant and human eukaryotic cell systems. Int J Mol Sci 24:13052. https://doi.org/10.3390/ijms241713052

Gupta DK, Huang HG, Nicoloso FT et al (2013) Effect of Hg, as and Pb on biomass production, photosynthetic rate, nutrients uptake and phytochelatin induction in *Pfaffia glomerata*. Ecotoxicology 22:1403–1412. https://doi.org/10.1007/s10646-013-1126-1

Gupta DK, Nicoloso FT, Schetinger MR et al (2011) Lead induced responses of *Pfaffia glomerata*, an economically important Brazilian medicinal plant, under in vitro culture conditions. Bull Environ Contam Toxicol 86:272–277. https://doi.org/10.1007/s00128-011-0226-y

Hansen CC, Nelson DR, Møller BL, Werck-Reichhart D (2021) Plant cytochrome P450 plasticity and evolution. Mol Plant 14:1244–1265. https://doi.org/10.1016/j.molp.2021.06.028

Heath RL, Packer L (1968) Photoperoxidation in isolated chloroplasts. Arch Biochem Biophys 125:189–198. https://doi.org/10.1016/0003-9861(68)90654-1

Hossain A, Maitra S, Sarker S et al (2023) Aluminium stress in plants: consequences and mitigation mechanisms. Beneficial Chemical Elements Of Plants: Recent Developments and Future Prospects 123–168. https:10.1002/9781119691419ch6

Huang C-F, Ma Y (2025) Aluminum resistance in plants: a critical review focusing on STOP1. Plant Commun 6:101200. https://doi.org/10.1016/j.xplc.2024.101200

Jiang X, Li H, Wang T et al (2012) Gibberellin indirectly promotes chloroplast biogenesis as a means to maintain the chloroplast population of expanded cells. Plant J 72:768–780. https://doi.org/10.1111/j.1365-313x.2012.05118.x

Kamada T, Picoli EAT, Alfenas AC et al (2009) Diversidade genética de populações naturais de Pfaffia glomerata (Spreng.) Pedersen estimada por marcadores RAPD. Acta Sci Agron 31. https://doi.org/10.4025/actasciagron.v31i3.548

Kar D, Pradhan AA, Datta S (2021) The role of solute transporters in aluminum toxicity and tolerance. Physiol Plantarum 171:638–652. https://doi.org/10.1111/ppl.13214

Karnovsky MJ (1965) A formaldehyde-glutaraldehyde fixative of high osmolality for use in electron microscopy. J Cell Biol 27:137–138A

Kesawat MS, Satheesh N, Kherawat BS et al (2023) Regulation of reactive oxygen species during salt stress in plants and their crosstalk with other signaling molecules-current perspectives and future directions. Plants 12:864. https://doi.org/10.3390/plants12040864

Kochian LV, Piñeros MA, Liu J, Magalhães JV (2015) Plant adaptation to acid soils: the molecular basis for crop aluminum resistance. Ann Rev Plant Biol 66:571–598. https://doi.org/10.1146/annurev-arplant-043014-114822

Lisec J, Schauer N, Kopka J, Willmitzer L, Fernie AR (2006) Gas chromatography mass spectrometry-based metabolite profiling in plants. Nat Protoc 1:387–396. https://doi.org/10.1038/nprot.2006.59

Livak KJ, Schmittgen TD (2001) Analysis of relative gene expression data using real-time quantitative PCR and the 2−ΔΔCT method. Methods 25:402–408. https://doi.org/10.1006/meth.2001.1262

Louback E, Batista DS, Pereira TAR (2021) CO_2 enrichment leads to altered cell wall composition in plants of *Pfaffia glomerata* (Spreng.) Pedersen (amaranthaceae). Plant Cell Tiss Org Cult 145:603–613. https://doi.org/10.1007/s11240-021-02031-4

Malavolta E, Vitti GC, Oliveira SA (1997) Assessment of nutritional status of plants principles and applications. 2nd edition, POTAFOS, Piracicaba- references - scientific research publishing. (n.d.). Scirp.org. https://www.scirp.org/reference/referencespapers?referenceid=1270262. Retrieved July 24, 2024, from

Maldaner J, Nicoloso FT, Tabaldi LA et al (2015) Aluminum accumulation in two *Pfaffia glomerata* genotypes and its growth effects. Cienc Rural 45:1013–1020. https://doi.org/10.1590/0103-8478cr20140439

Manquián-Cerda K, Cruces E, Escudey M, Zúñiga G, Calderón R (2018) Interactive effects of aluminum and cadmium on phenolic compounds, antioxidant enzyme activity and oxidative stress in blueberry (*vaccinium corymbosum* L.) plantlets cultivated *in vitro*. Ecotoxicol Environ Saf 150:320–326. https://doi.org/10.1016/j.ecoenv.2017.12.050

Nascimento EX, Mota JH, Vieira MC, Zárate NAH (2007) Biomass production of *Pfaffia glomerata* (Spreng.) Pedersen and *plantago major* L. in single and intercropping. Cienc Agrotecnol 31:724–730. https://doi.org/10.1590/s1413-70542007000300019

Nunes-Nesi A, Carrari F, Gibon Y et al (2007) Deficiency of mitochondrial fumarase activity in tomato plants impairs photosynthesis via an effect on stomatal function. Plant J 50:1093–1106. https://doi.org/10.1111/j.1365-313x.2007.03115.x

O'Brien TP, McCully ME (1981) The study of plant structure principles and select methods. Termacarphi Ltda 56–58

Panda SK, Baluška F, Matsumoto H (2009) Aluminum stress signaling in plants. Plant Signal Behav 4:592–597. https://doi.org/10.4161/psb.4.7.8903

Phukunkamkaew S, Tisarum R, Pipatsitee P et al (2021) Morpho-physiological responses of indica rice (*oryza sativa* sub. indica) to aluminum toxicity at seedling stage. Environ Sci Pollut Res Int 28:29321–29331. https://doi.org/10.1007/s11356-021-12804-1

Rahman R, Upadhyaya H (2021) Aluminum toxicity and its tolerance in plant: a review. J Plant Biol 64:101–121. https://doi.org/10.1007/s12374-020-09280-4

Ranjan A, Sinha R, Lal SK, Bishi SK, Singh AK (2021) Phytohormone signalling and cross-talk to alleviate aluminium toxicity in plants. Plant Cell Rep 40:1331–1343. https://doi.org/10.1007/s00299-021-02724-2

Renault H, Alber A, Horst NA et al (2017) A phenol-enriched cuticle is ancestral to lignin evolution in land plants. Nat Commun 8:1–8. https://doi.org/10.1038/ncomms14713

Sade H, Meriga B, Surapu V et al (2016) Toxicity and tolerance of aluminum in plants: tailoring plants to suit to acid soils. BioMetals 29:187–210. https://doi.org/10.1007/s10534-016-9910-z

Sami A, Shah FA, Abdullah M et al (2020) Melatonin mitigates cadmium and aluminum toxicity through modulation of antioxidant potential in *Brassica napus* L. Plant Biol 22:679–690. https://doi.org/10.1111/plb.13093

Silva TD, Batista DS, Castro KM et al (2021) Irradiance-driven 20-hydroxyecdysone production and morphophysiological changes in *Pfaffia glomerata* plants grown in vitro. Protoplasma 258:151–167. https://doi.org/10.1007/s00709-020-01558-1

Singh S, Tripathi DK, Singh S et al (2017) Toxicity of aluminum on various levels of plant cells and organism: a review. Environ Exp Bot 137:177–193. https://doi.org/10.1016/j.envexpbot.2017.01.005

Sousa A, AbdElgawad H, Fidalgo F et al (2020) Al exposure increases proline levels by different pathways in an Al-sensitive and an Al-tolerant rye genotype. Sci Rep 10:1–11. https://doi.org/10.1038/s41598-020-73358-9

Spormann S, Soares C, Teixeira J, Fidalgo F (2021) Polyamines as key regulatory players in plants under metal stress-A way for an enhanced tolerance. Annals Appl Biol 178:209–226. https://doi.org/10.1111/aab.12660

Sun C, Lv T, Huang L et al (2020) Melatonin ameliorates aluminum toxicity through enhancing aluminum exclusion and reestablishing redox homeostasis in roots of wheat. J Pineal Res 68(4). https://doi.org/10.1111/jpi.12642

Szabados L, Savouré A (2010) Proline: a multifunctional amino acid. Trends Plant Sci 15:89–97. https://doi.org/10.1016/j.tplants.2009.11.009

Umar AW, Naeem M, Hussain H, Ahmad N, Xu M (2025) Starvation from within: how heavy metals compete with essential nutrients, disrupt metabolism and impair plant growth. Plant Sci 353:112412. https://doi.org/10.1016/j.plantsci.2025.112412

Ur Rahman S, J-C H, Ahmad M et al (2024) Aluminum phytotoxicity in acidic environments: a comprehensive review of plant tolerance and adaptation strategies. Ecotoxicol Environ Saf 269:115791. https://doi.org/10.1016/j.ecoenv.2023.115791

Watanabe T, Osaki M, Yano H, Rao IM (2006) Internal mechanisms of plant adaptation to aluminum toxicity and phosphorus starvation in three tropical forages. J Plant Nut 29:1243–1255. https://doi.org/10.1080/01904160600767484

Wellburn AR (1994) The spectral determination of chlorophylls a and b, as well as total carotenoids, using various solvents with spectrophotometers of different resolution. J Plant Physiol 144:307–313. https://doi.org/10.1016/s0176-1617(11)81192-2

Weng J-K, Chapple C (2010) The origin and evolution of lignin biosynthesis. New Phytol 187:273–285. https://doi.org/10.1111/j.1469-8137.2010.03327.x

Zhang J, Li D, Wei J et al (2019) Melatonin alleviates aluminum-induced root growth inhibition by interfering with nitric oxide production in *Arabidopsis*. Environm Exp Bot 161:157–165. https://doi.org/10.1016/j.envexpbot.2018.08.014

Publisher's Note Springer Nature remains neutral with regard to jurisdictional claims in published maps and institutional affiliations.

Authors and Affiliations

Michelle Maylla V. Almeida[1,7] · Tatiane D. Silva[1,7] · Quezia P. Dutra[1] · Luiza Eduarda G. Monteiro[1] · Marcus Dhilermando H. Souza[1] · Elisandra S. Sousa[1] · Joseila Maldaner[2] · Sérgio Heitor S. Felipe[3] · Juliane M. Henschel[4] · Diego S. Batista[4,6] · Evandro A. Fortini[1,7] · Auxiliadora O. Martins[5] · Wagner L. Araújo[5] · Wagner C. Otoni[1]

✉ Diego S. Batista
diegoesperanca@gmail.com

✉ Wagner C. Otoni
wotoni@ufv.br

[1] Departamento de Biologia Vegetal/Laboratório de Cultura de Tecidos Vegetais/BIOAGRO, Campus Universitário, Universidade Federal de Viçosa, Viçosa, MG 36570-900, Brazil

[2] Departamento de Diagnóstico e Pesquisa Agropecuária, Centro Estadual de Diagnóstico e Pesquisa Florestal (CEFLOR), Santa Maria, RS 97001-970, Brazil

[3] Universidade Federal Rural da Amazônia, Capitão Poço, PA 68650-000, Brazil

[4] Programa de Pós-graduação em Agronomia, Universidade Federal da Paraíba, Areia, PB 58397-000, Brazil

[5] National Institute of Science and Technology on Plant Physiology Under Stress Conditions, Departamento de Biologia Vegetal, Universidade Federal de Viçosa, Viçosa, MG 36570-900, Brazil

[6] Department of Agriculture, Federal University of Paraíba, University Campus III, s/n, Bananeiras, PB 58220-000, Brazil

[7] Present address: CTC - Centro de Tecnologia Canavieira - CTC, Piracicaba, SP 13.400-970, Brazil